Acta Microscópica Vol. 29, No. 1, 2020, pp. 97 – 105
Special issue Microscopy on Corrosion

Surface Morphology of Air Plasma Sprayed Titania doped Yttria stabilized Zirconia Coatings

S. Liscano[1]*, E. Medina[1], M. Romero[1], L. Gil[1]

[1] Universidad Nacional Experimental Politécnica "Antonio José de Sucre" Departamento de Ingeniería Metalúrgica, Urb. Villa Asia, Puerto Ordaz, Venezuela.

Corresponding Autor: E-mail: sliscano@unexpo.edu.ve, phone/fax: +58-286-9624595

ABSTRACT
In this research, the influence of the projection parameters on the surface morphology of ZrO_2-10% Y_2O_3-18% TiO_2 coatings thermal sprayed by atmospheric plasma was determined. To do this, the surface morphology was characterized by Scanning Electron Microscopy for different conditions of deposition (Input Power and Spray Distance), the percentage of unmelted particles and porosity were simultaneously determined by image analysis, as well as the surface roughness of each coating. Finally, the influence of the projection parameters was established by means of a 2^2 factorial experimental design and analysis of variance, optimizing the results using a response surface methodology. The coatings presented an overlaid splats morphology with the presence of unmelted particles and a certain degree of porosity. It was found that with higher input power and shorter spray distance, a more homogeneous structure is obtained with fewer discontinuities (unmelted particles, porosity, roughness). The combined effect of the input power and the spray distance evaluated determines that the most favorable experimental combination achieves when the coating of ZrO_2-10%Y_2O_3-18% TiO_2 is deposited with a power of 38 kW and a spray distance of 80 mm.

Keywords: ZrO_2-10% Y_2O_3-18% TiO_2, APS Coatings, Porosity, Roughness, Unmelted Particles

Morfología Superficial de Recubrimientos Termorrociados por Plasma de Zirconia estabilizada con Ytria dopados con Titania

RESUMEN
En esta investigación, se determinó la influencia de los parámetros de proyección en la morfología superficial de recubrimientos ZrO_2-10% Y_2O_3-18% TiO_2 termorrociados por plasma atmosférico. Para ello, se caracterizó mediante Microscopía Electrónica de Barrido la morfología superficial para distintas condiciones de deposición (Potencia de Entrada y Distancia de Rociado), de manera simultánea, se determinó el porcentaje de partículas no fundidas y la porosidad mediante análisis de imagen, así como la rugosidad superficial de cada uno de los recubrimientos. Por último, se correlacionaron los parámetros de proyección mediante un diseño de experimentos factorial 2^2 y análisis de varianza, optimizándose los resultados mediante la metodología de superficies de respuesta. Estos recubrimientos presentaron una morfología lamelar con presencia de partículas no fundidas y bajo porcentaje de porosidad. Se determinó que a mayor potencia de entrada y menor distancia de rociado se obtiene una estructura más homogénea y con menos discontinuidades (partículas no fundidas, porosidad, rugosidad). El efecto combinado de la potencia de entrada y distancia de rociado evaluados, determina que la combinación experimental más favorable se logra cuando se deposita el recubrimiento de ZrO_2-10% Y_2O_3-18% TiO_2 con una potencia de 38 kW y una distancia de rociado de 80 mm.

Palabras clave: ZrO_2-10% Y_2O_3-18% TiO_2, Recubrimientos termorrociados, Porosidad, Rugosidad, Partículas no fundidas.

INTRODUCTION

The application of coatings is a common practice, as many metal structures and parts are currently subjected to severe service conditions. Ceramic coatings stand out for their excellent properties, these are frequently used to protect surfaces from damage that can be caused by wear or corrosion in environments at high temperatures [1]. These coatings can be applied by thermal spraying, in which the molten particles of ceramic material project at high speeds (up to 500 m/s), embedding themselves and forming between them a dense coating and strongly adhered to the substrate [1-2].

The microstructure of plasma sprayed ceramic coatings is commonly constituting by successive layers of splats adhere to each other and to the substrate, but also are some defects like pores, unmolten or partially melted particles and cracks that affect the mechanical, physical and chemical properties of the coatings [3].

In previous authors researches [4-5], have been stablished that microstructural characteristics of these coatings depend on the feed materials and the projection parameters used during the manufacturing process, and they reported correlations for microstructural aspects measure on transversal sections of coatings.

The present work was undertaken to study the effects of power input and spray distance on the surface morphology of air plasma spraying Titania Doped Yttria Stabilized Zirconia Coatings. The effect of variation in power input and spray distance was studied for coatings through 2^2 factorial experimental design (four conditions and the powder fabricant practice recommended) with respect to the changes in percentage of unmelted particles, percentage of porosity, and surface roughness of the coatings, all evaluate since of coatings surface.

MATERIALS AND METHODS

ASTM A36 steel bars with a calibrated section of 20 × 50 mm in length, shot blasted with Al_2O_3 size 0-1, were industrially coated with agglomerate powder of ZrO_2-10%Y_2O_3-18%TiO_2 (Metco 143, Sulzer Metco, Westbury, NY), of 75 ± 5 µm particle size, using a TAFA model G-100 plasma gun, a powder feed rate of 54 g/min and 75 Standard Cubic Feet per Hour (SCFH) of Ar rate (primary) and 15 SCFH of H_2 rate (secondary).

The fabrication of coatings was carried out following the experimental runs show in the table I.

Table I. Experimental runs used for the deposition of coatings.

Run	Input Power	Spray distance	Input power (kW)	Spray distance (mm)
1	-	-	32	80
2	+	-	38	80
3 *	0	0	35	100
4	-	+	32	120
5	+	+	38	120

***** Run 3 is the powder fabricant practice recommended.

Scanning Electron Microscopy and Image Analysis.

The coating surface morphology was examined using a FEI scanning electron microscope model Quanta 200, in mixed mode. The percentages of unmelted particles and porosity were carried out by the use of Image J software (Image J is free open source software for images processing) using as reference the Standard Test Methods for Determining Area Percentage Porosity in Thermal Spray Coatings (ASTM E2109) [6]. The difference in the procedure used to measure the unmelted particles was on the thresholding step, where the spherical form and brighter gray were considering as the criteria for threshold the unmelted particles (figure 1).

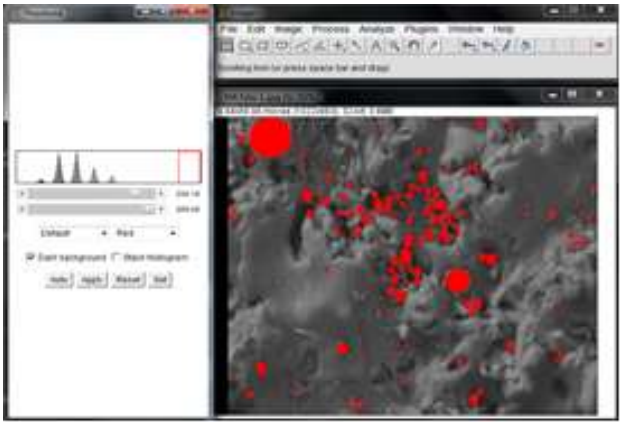

Fig. 1a. Screenshots for Image J operations: Red mask during thresholding step

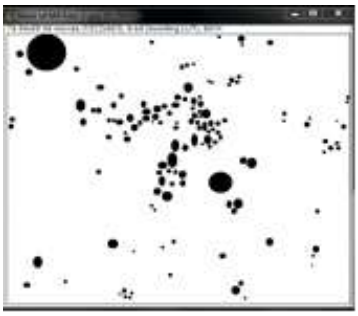

Fig. 1b. Screenshots for Image J operations: Resulting binary image.

The phases present in the coatings were characterized by microanalysis EDS and X Ray Diffraction (XRD) in previous research of authors [5].

Measurement of Surface Roughness.

A Mitutoyo rugosimeter model SJ 400 with inductive probe roughness with a diamond tip of 5 µm radius was used; with a measurement capacity of up to 800 µm. Three (3) measurements were made for each condition obtaining the roughness profile and Ra value. The roughness tests were performed at an evaluation length of 10 mm, in accordance with Surface Roughness Standard: JIS B 0601-2013 [7].

Analysis of Variance and Response Surface Model.

The computational package Statgraphics [8] was used to carry out an analysis of variance in order to determine the importance of one or more factors and the interactions of them when comparing the means of the response variable at the different levels of factors and secondly, the response surface methodology was applied to determine the conditions that offer the best coatings properties, between the level of the variables studied in this work.

RESULTS AND DISCUSSION

Scanning Electron Microscopy of the ceramic coatings and Image Analysis.

In the Figure 2a of run 1 (32 kW, 80 mm), showing the micrograph of as-sprayed coating surface, is possible distinguish the presence of micro particles and agglomerates of nanoparticles in condition unmelted, with different morphology, forthcoming of powder agglomerate, beside of a layered splat structure, rounded by pores and intersplat cracks [3]. These microstructural characteristics indicate that the powder particle did not reach the semimolten condition necessary to produce a complete layered splat structure [9].

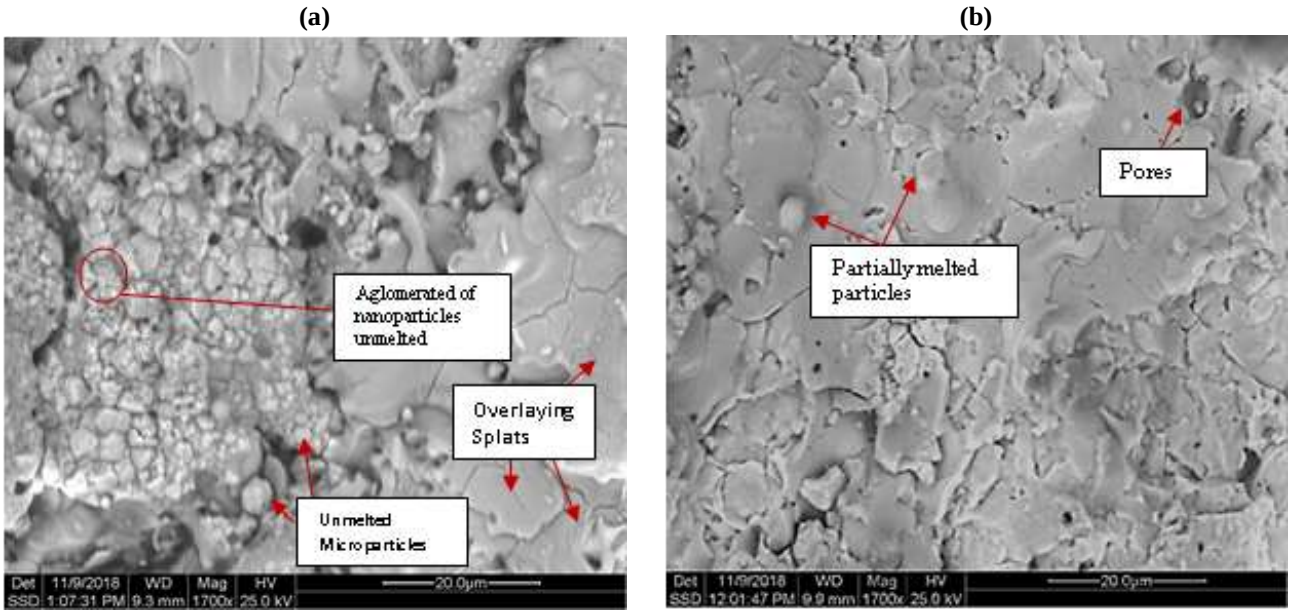

Fig. 2. SEM images of coatings surface (BSE, 1700X). (a) Run 1 (32kW, 80 mm), (b) Run 2 (38 kW, 80 mm).

For run 2, (38 kW, 80 mm) in the Figure 2b, a more cohesive surface microstructure is observed, with little presence of partially melted particles and pores. The layered splat structure can be distinguished through of overlaying splashes of completely molten and flattened particles. These characteristics are maintained over the entire surface of the sample of this run, which correspond to typical microstructure of plasma spray ceramics coatings.

In figure 3, the micrographs of surface coatings for runs 3, 4 and 5 are showed. There, are possible find similar microstructure characteristics: spherical particles overlays in a layered splat structure, around of big pores and unfilled voids. All of these considered defects or discontinuities of coatings [3]. The unmelted particles keep the spherical form from the agglomerated powder; originate a quite anisotropic microstructure that became, as centers of secondary defects degrading the functional properties of the coatings [9].

As the spherical form is the principal attribute of unmelted particles [9], in the table 2 are presented the image analysis results for unmelted particles percentage in the coatings for each condition. There, it can be seen that run 2 has the lowest percentage of unmelted particles (0.29 %) and the most unfavorable condition turned out to be run 1, with 5.78 % unmelted particles. From this results, it can be inferred that the input power has an inversely relationship with % unmelted particles.

Table 2. Image analysis results of coatings surface.

Run	%Unmelted Particles	%Porosity	Roughness, Ra (µm)
1	5.78 ± 0.49	7 ± 2.8	7.24 ± 0,18
2	0.29 ± 0.05	2 ± 1.1	5.33 ± 0.15
3	4.54 ± 0.94	5 ± 0.5	6.65 ± 0.09
4	3.48 ± 0.51	8 ± 1.3	5.74 ± 0.34
5	2.76 ± 0.30	6 ± 1.4	5.43 ± 0.18

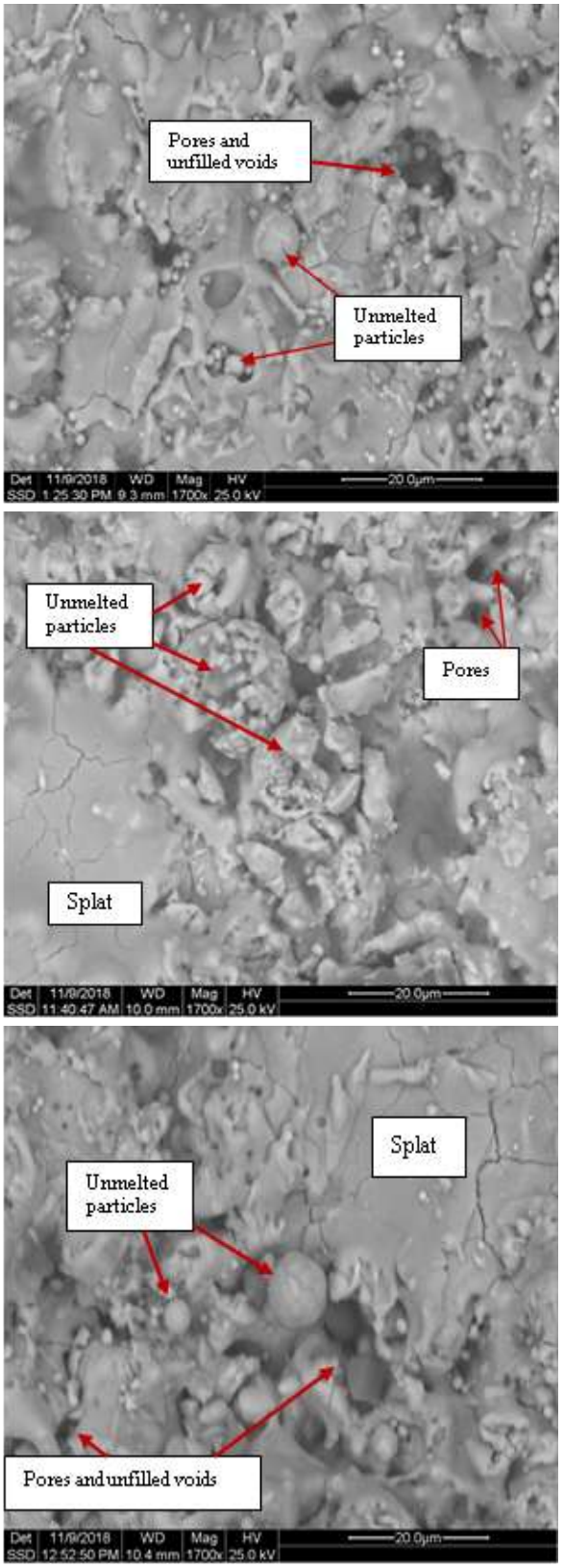

Fig. 3. SEM images of coatings surface (BSE, 1700X) a) Run 3 (35kW, 100 mm), b) Run 4 (32kW, 120 mm), c) Run 5 (38kW, 120 mm).

At low input power the powder particles are poorly melted, and when they impact on the substrate are not able to spread out completely to form the splats. When the input power is high, most of the powder particles are completely melted and the flow ability to form splats is good [10]. In the table 2, also is present the results of the % porosity for each condition. Figure 4 shows binary images of the porosity, from Image J software, used for determine the % porosity on the coatings, showing the distribution of pores in three sections of coatings surface, for each condition.

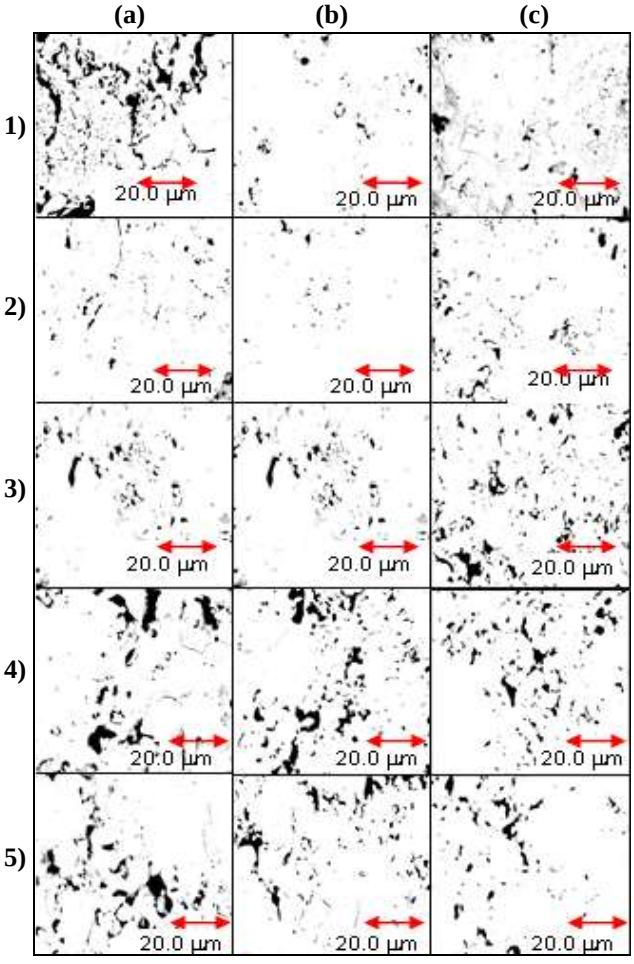

Fig. 4. Binary images from SEM images analysis used to determine the % porosity in three sections (a, b, c) for each condition. 1) 32kW, 80 mm, 2) 38 kW, 80 mm, 3) 35kW, 100 mm, 4) 32kW, 120 mm, 5) 38kW, 120 mm.

It's possible to observe an irregular morphology of the pores that meanly is associated to incomplete contact between contiguous splats [11] and the presence the unmelted particles and oxides [10-11]. The higher porosity is present in the run 4; which have the lowest input power (32 kW) and highest spray distance (120 mm). As discussed above, when the input power is relatively low, the content of unfused particles in the coating increases, therefore, during the cooling process after spraying, microcracks and pores will form close to the limit of the unfused particle. On the other hand, with a longer spraying distance, the pulverized powder has more time to react with the air entrained by the flame, which would lead to an increase in the oxide content with the spraying distance, and thus the porosity. [10]. Tillman [11] refers the microstructure of ceramic coatings exhibit globular pores, delaminations or interlamellar pores, and micro-cracks which compose the coating's porosity. The two last are related with the rapid splat solidification, high velocity impingement of the moltenparticles and relaxation of tensile quenching stresses.

Surface roughness.

The figure 5 presents the surface roughness profiles for the five conditions of coatings deposition and indicating the Ra value with its correspondent standard deviation.

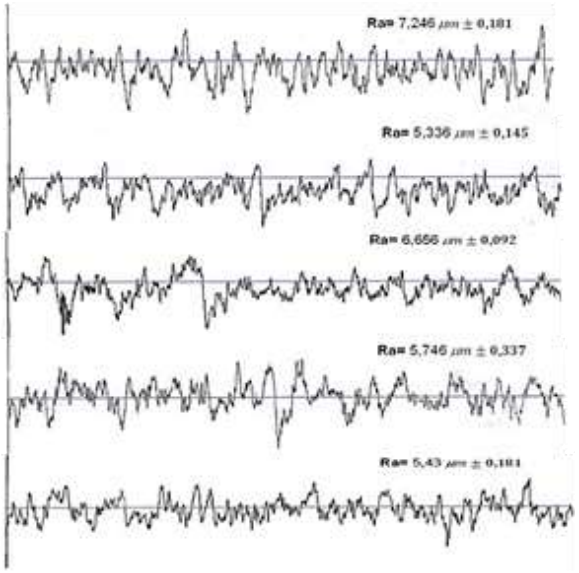

Fig. 5. Superficial Roughness Profiles of coatings.

The lowest mean roughness (Ra) was obtained for run 2, which had the lowest percentage of unmelted particles. The highest roughness turned out to be on run 1. The figure 6 also shows the roughness has not significative variation for runs 2, 4 and 5, whose have similar percentage of unmelted particles. These results allow inferred that exist a proportionally correlation between surface roughness and the unmelted particles [1].

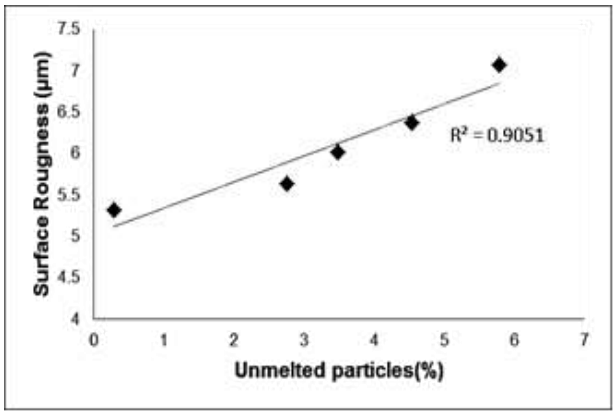

Fig. 6. Correlations between surface roughness and the porcentage Unmelted particles.

The Figure 6 shows that exist a good linear correlation for surface roughness and the % unmelted particles. When the % unmelted particle is high, numerous spherical particles are present on the surface of coatings; incrementing the amount and height of peaks in the roughness profile; therefore the Ra value is higher. In this case, the valley portions in the roughness profile are representing the layered splat structure that constitutes the coating. However, the Ra results for all runs are considerably lower than the reported by Kar [1] for ceramic coatings systems of ytria stabilized zirconia deposited using atmospheric plasma spray.

Analysis of Variance and Response Surface Model. According to the analysis of variance, influence of the input power and the spray distance on the unmelted particles, the porosity and surface roughness are not pronounced in the evaluated study range, however they do generate a certain effect which is described.

An analysis of variance (ANOVA) was performed, in a 95% confidence interval to establish the effect of the factors on the response variables, see Figure 7.

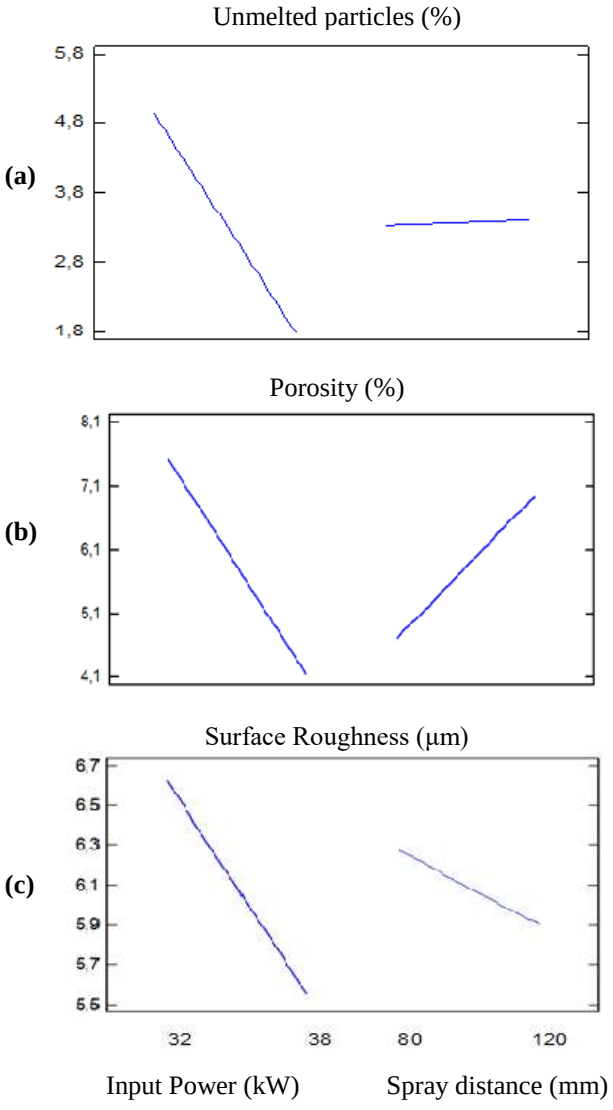

Fig. 7. Main effects by influencing variables on (a) Unmelted particles (%), (b) Porosity (%), (c) Surface Roughness.

The R-Square statistic indicated that the model explains 90% of the variability in unmelted particles.

In Figure 7a, we can see the graphs of the main effects for the unmelted particles, where the higher the value of the slope of the line, the greater the significance of the factor

in the unmelted particles. In this case, the spray distance has a slope of the line with a low value, so this variable does not have a great influence on the range of study of this investigation. Findings similar were reported by Kucuk [13] for yttria stabilized zirconia coatings. However, the input power is a factor with great significance due to its steep slope, finding that the higher the input power, the lower the percentage of unmelted particles will be on the surface of the coating.

These results are in line with previous works of authors [5] and Karthikeyan [12], whose affirm that the power contributes the energy required to melt the powders and its increase favors the temperatures of the particles and with it their fusion. The R-Square statistic indicated that the model explains 97% of the variability in Porosity.

In figure 7b, the graphs of the main effects for porosity can be observed, where both lines indicate a great significance of the factors. In this case, the input power has an inverse relationship with the porosity, that is, the higher the power, the less porosity, while the spray distance has a direct relationship with the porosity, that is, the greater the distance, the greater the porosity that will result in the coating.

The R-Square statistic indicated that the model explains 94% of the variability in Porosity. In figure 7c, it can be distinguished the graphs of the main effects for surface roughness, the line of the effect of the input power is the most significant, therefore to higher the input power the surface roughness is lower of the coating. The spray distance has little influence on the roughness, with a slope close to zero (-0.3).

In order to establish the values of the factors that optimize those of the response variables, a response surface model (RSM) was performed [4], in this way the optimal operating projection parameters in the atmospheric plasma spray process will be determined in ZrO2-10% Y2O3-18% TiO2 coatings.

Figure 8 shows the response surface that helps determine the combination of experimental factors that simultaneously optimize the values of the response variables. In this case, the goals that were set are to try to minimize the content of unmelted particles, the porosity and the surface roughness of the coating, resulting in the highest desirability of 0.880 for an input power of 38 kW and a spray distance of 80 mm corresponding to condition 2 in this study. This indicates that it is the most favorable condition for depositing and optimizing the surface characteristics of the ZrO_2 - 10% Y_2O_3 - 18% TiO_2 coating.

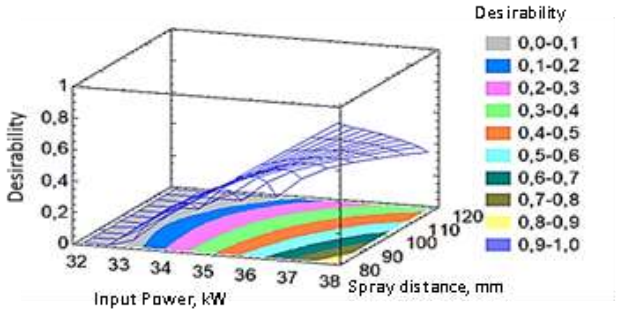

Fig. 8. Estimated Response Surface for Multiple Response Optimization.

CONCLUSIONS

The surface morphology of the ZrO_2-10% Y_2O_3-18% TiO_2 coatings is principally overlaying splashing of molten particles, with the presence of unmelted particles, porosity and some intersplat cracks. The experimental condition that accurate the lowest percentage of unmelted particles and porosity corresponded to condition 2 (Power 38 kW and Distance 80 mm) with 0.29 ± 0.05 and 2 ± 1,1 respectively. The most unfavorable condition turned out to be condition 1 (Power 32 kW and Distance 80 mm) with 5.78 ± 0.5 percent of unmelted particles and 7±2.8 percent of porosity. The surface roughness was greater for condition 1 (7.08 ± 0.18) and the lowest for condition 2 (5.33 ± 0.15). However, there is not a very marked variation in the range of study of this research. The

percentage of unmelted particles is closely related to the surface roughness of the coating.

For its part, the input power is the most significant parameter in the surface morphology of the coating, while the spray distance is of less influence. The combined effect of the input power and the spray distance evaluated determine that the most favorable experimental combination is achieved, when the coating of ZrO_2-10% Y_2O_3-18% TiO_2 is deposited with a power of 38 kW and a spray distance 80 mm.

ACKNOWLEDGEMENTS

To Project PEII N° 201100001089 titulad "Fabricación y Evaluación de Recubrimientos Cerámicos Termorrociados para Aplicaciones a Altas Temperaturas en Componentes de Reactores de Reducción Directa, MPPEUCT, Venezuela.

Institute of Research in Materials and Metallurgy of SIDOR, Puerto Ordaz, Venezuela.

REFERENCES

[1] Kar S., Paul S. Bandyopadhyay P. P. (2016) "Processing and characterization of plasma sprayed oxides: Microstructure, phases and residual stress" *Surf. Coat. Technol.* 304:364-374. DOI: 10.1016/j.surfcoat.2016.07.043.

[2] Tejero-Martin D., Rad M. R., McDonald A. Hussain T. (2019) "Beyond traditional coatings: A review on thermal-sprayed functional and smart coatings" *J. Therm. Spray Technol.* 28(4):598-644. DOI: 10.1007/s11666-019-00857-1.

[3] Odhiambo J. G., Li W., Zhao Y., Li C. (2019) "Porosity and its significance in plasma-sprayed coatings" *Coatings* 9(7):460. DOI: 10.3390/coatings9070460.

[4] Liscano S., Padilla P., Romero M., Gil L. (2016) "Optimización de los parámetros de deposición por termorrociado por plasma atmosférico de recubrimientos de NiCrAlCoYO usados como capa de anclaje en sistemas barreras térmicas", *Acta Microscópica*, 25(1): 9-15.

[5] Liscano S., Gil L., Cabanzo R., Mejía E. (2018) "Microestructura de recubrimientos ZrO_2-10%Y_2O_3-18%TiO_2 termorrociados por plasma atmosférico" *Revista de la Facultad de Ingeniería U.C.V.* 33(2):59-70.

[6] Asociación Americana de Ensayo de Materiales. (2014) *"*Standard Test Methods for Determining Area Percentage Porosity in Thermal Sprayed Coatings*"* (ASTM International, E2109-01).

[7] Japanese Standards Association. (2013) "Geometrical Product Specifications (GPS) - Surface texture: Profile method - Terms, definitions and surface texture parameters" (JIS B 0601).

[8] Statgraphics Plus version 5.1. (2001) Statistical Graphics Corporation.

[9] Ctibor P., Roussel O., Tricoire A. (2003) "Unmelted particles in plasma sprayed coatings" *J. Eu. Ceram. Soc.* 23(16):2993-2999. DOI: 10.1016/S0955-2219(03)00104-3.

[10] Thirumalaikumarasamy D., Shanmugam K., Balasubramanian V. (2012) "Influences of atmospheric plasma spraying parameters on the porosity level of alumina coating on AZ31B magnesium alloy using response surface methodology" *Prog. Nat. Sci: Materials International* 22(5):468-479. DOI: 10.1016/j.pnsc.2012.09.004.

[11] Tillmann W., Khalil O. Abdulgader M. (2019) "Porosity Characterization and Its Effect on Thermal Properties of APS - Sprayed Alumina Coatings" *Coatings* 9(10):601. DOI: 10.3390/coatings9100601.

[12] Karthikeyan S., Balasubramanian V. Rajendran, R. (2014) "Developing empirical relationships to estimate porosity and microhardness of plasma-sprayed YSZ coatings" *Ceram. Int.* 40(2):3171-3183. DOI: 10.1016/j.ceramint.2013.09.125.

[13] Kucuk A., Berndt C. C., Senturk U., Lima R. S. Lima C. R. C. (2000) "Influence of plasma spray parameters on mechanical properties of yttria stabilized zirconia coatings. I: Four point bend test" *Mater. Sci. Eng. A* 284(1-2):29-40. DOI: 10.1016/S0921-5093(00)00799-1.